UNITED STATES AIR FORCE
AIR UNIVERSITY
AIR FORCE INSTITUTE OF TECHNOLOGY
Wright-Patterson Air Force Base, Ohio

ELECTRICAL EFFECTS OF SNOW
AND ICE COATINGS ON
REFLECTOR ANTENNAS

WILLIAM A. DAVIS
Capt   USAF

Assistant Professor of
Electrical Engineering
Technical Report - AFIT TR 77-8
December 1977

DDC

RECEIVED
JAN 23 1978

See 1473   012200

ACKNOWLEDGEMENT

TABLE OF CONTENTS

LIST OF FIGURES

ELECTRICAL EFFECTS OF SNOW AND ICE COATINGS ON REFLECTOR ANTENNAS

William A. Davis

AIR FORCE INSTITUTE OF TECHNOLOGY
Department of Electrical Engineering
Wright-Patterson AFB, Ohio 45433

ABSTRACT

In recent years, the effects of icing on reflector antenna systems used in precision approach radars has become an ever increasing problem of interest. This paper presents a simple technique that may be used for the analysis of the icing on such reflector systems. For simplicity, the ice is assumed to have a uniform vertical thickness over the upper side of exposed surfaces.

Beginning with a uniform phase front in the beam direction for the uniced reflector, one can trace rays back to the reflector using geometrical optics to determine the angle of incidence at each point on the reflector. The phase and amplitude of the rays for the iced reflector are computed by local plane wave analysis and used to calculate the far field in the manner of physical optics. This technique gives downward beam shifts of up to 30 milliradians for some typical reflectors.

This technique modifies the array aperture function. The full pattern can be obtained from the convolution of the computed pattern with the pattern of the original system.

ELECTRICAL EFFECTS OF SNOW AND ICE COATINGS IN REFLECTOR ANTENNAS

by

William A. Davis

AIR FORCE INSTITUTE OF TECHNOLOGY
Department of Electrical Engineering
Wright-Patterson AFB, Ohic   45433

August 1977

Technical Report

1.0 INTRODUCTION

In recent years the Air Force has become increasingly concerned
with runway operations under all types of weather conditions. To meet
the requirements posed by adverse weather conditons, Raytheon Company
has developed two precision approach radars (PAR). One of these was
designed for portable use and the other for fixed use. However, they
.both are very similar and can be analyzed in like manners.

To operate under adverse weather conditions, several features were
designed into these PAR antenna systems. The primary feature of rain
cancellation was built in by using circular polarization. To understand
this feature, consider a spherical model of rain drops. In receiving the
opposite circular polarization as simple reflection theory would suggest,
substantial rain clutter is encountered. However, the rain clutter, due
to the spherical symmetry of rain drops, is substantially reduced by
using the same polarization. Though certain geometries reflect primarily
the opposite circular polarization, typical aircraft reflect a sufficient
amount of energy with the same polarization to gain a significant clutter
advantage.

1

The electrical effects of water, snow, and ice on the feeds of these reflector antennas was eliminated by orienting the feeds downward and providing drainage for any condensation. The mechanical effects of ice loading on both the feed and the reflector were compensated for structurally.

The only effects that were not accounted for were the effects of ice or snow buildup on the electrical characteristics of the reflector surface. Two preliminary studies by E. Tippie (1976) and by Dr. R. J. Mailloux (1976) suggested that this should be an effect of great concern, especially for the use of these PAR's in colder climate areas. The purpose of this report is to study this phenomenon in more detail for the antenna systems of interest to both confirm the previously reported data and to obtain estimates of the extent of the effects for various conditions of ice and snow.

We will first develop the theory of the antenna analysis based on the theories of geometrical optics and physical optics and discuss the properties of ice and snow at radar frequencies. Lastly we shall apply the theory to the two antenna systems developed by Raytheon for several cases of interest and draw our conculsions based on these results.

2.0 THEORETICAL DEVELOPMENT

The theory used for analysis in this report is a combination of geometrical optics and physical optics. To give a more complete picture of how this applies to the antenna systems of interest, we will first review the analyses of these systems as done by Raytheon Company and then present the method used to consider the electrical effects of snow and ice buildup on the reflector.

2.1 DESIGN ANALYSIS

The basic design of the systems is described in the Critical Design Review (CDR) on the TPN-19 and is reviewed in a paper by L. Meloncon (197X). For clarity, the pertinent portions are repeated below.

The first step in the design was the choice of reflector surface. This choice was made by studying the beamwidth properties of various reflector geometrics versus scan angle. Geometrical optics* was used to trace rays from a fixed set of points in a feed array to the reflector and on in the direction of desired scan. The ray intersections with the reflector retained the most uniform pattern for a hyperbolic surface. The resultant conclusion of uniformity of the main beam antenna pattern shape versus scan lead to the choice of a hyperbolic conic section as the reflector in both antenna systems.

The feed array was chosen to exist of a monopulse waveguide horn illuminating a transmission array either directly or reflectively. The transmission array is an array of individual waveguide phase shifter elements followed by polarizers used to convert linear polarization to circular polarization. The phasing of the elements controls the direction of the main beam and is determined by an approximate formula for each

---

*This may be thought of as the tracing of light (electromagnetic) beams.

3

element. These formulae were obtained by tracing rays from a uniform wavefront in the scan direction back to each element after reflection from the reflector using geometrical optics.

Since the geometry and the phasing for desired scan angles are both known quantities, one can calculate the pattern of the antenna systems for given scan angles. To use geometrical optics for this task, one obtains the phases of the array elements and traces a ray from each element to a distant point in some direction. Summing all of these rays, including element phases and phases of the different path length delays of the rays, and repeating the summation for many other directions, one is able to construct the antenna pattern about a particular scan angle.

Raytheon chose the equally valid procedure of physical optics for calculating the antenna pattern of the antenna system. After determining the phasing of the feed array, the magnetic field, $\overline{H}^{inc}$, at the surface of the reflector is calculated as if the reflector were absent. The physical optics procedure is then used to estimate the current on the reflector surface as

$$\overline{J}_s = 2\hat{n} \times \overline{H}^{inc} \tag{1}$$

where $\hat{n}$ is the normal to the reflector and is oriented toward the feed. The antenna pattern is given by the magnitude of

$$\overline{P} = A \int\limits_{\substack{\text{Reflector} \\ \text{Surface}}} (\hat{r} \times \overline{J}_s) \, e^{jk\hat{r}\cdot\overline{r}'} \, ds'$$

where: $\hat{r}$ = direction of interest

$\overline{r}'$ = point on reflector surface

$k = 2\pi/$ (wavelength)

$A = 1/($Maximum magnitude of integral versus direction$)$

4

It should be pointed out that both of these methods are essentially equivalent and that neither includes the effects of diffraction by the edges of the reflector but only the effects of reflection (Kouyoumjian, 1965). Though the diffraction effects should be negligible, they could have been taken into account using the more rigorous theories of the geometrical theory of diffraction (GTD) or the physical theory of diffraction (PTD).

2.2 COATED REFLECTOR ANALYSIS.

The analysis of ice or snow buildup on the reflector surface may simply be cast as the problem of a reflector with a lossy dielectric coating. Since elevation error is of prime interest, the analysis has been done for the problem in two-dimensions. This is consistent with ignoring the effects of horizontal scan. The results for the GPN-XX fixed antenna system will have negligible variation from the vertical results of the three-dimension problem with a horizontally centered beam. In this case, the primary reflection is from the vertical center line of the reflector which can be modeled as an infinite hyperbolic cylinder with pattern variations only in the vertical direction.

The TPN-19 portable antenna system poses a slight problem due to the horizontal offset of the feed. To correctly account for this offset, the vertical angle that the ray makes with the reflector in the above analysis must be corrected by the offset. This angular correction has not been taken into account in the results presented. However, the results are a conservative estimate of the effects and as a consequence still serve as a reliable estimate of the problem with a dielectric thick-

5

ness of about 0.87 times that used for computation.

To determine the effect of the coating, we first assume that the antenna produces a planar phase front in the direction of scan. Tracing the rays back to the surface using geometrical optics, we are able to determine the angle of incidence with the surface of the reflector. This angle may be used to determine the attenuation and phase shift that would occur for a ray interacting with a dielectric coating at each point on the surface. The difficulty in analyzing three-dimensional problems involves this calcuation which is polarization dependent. Though tractable, it is not felt that the additional complication provides any insight beyond the two-dimensional problem.

The antenna pattern is calculated from these phase and amplitude modifications of a uniformly illuminated aperture and compared to the pattern with no modification. This procedure is akin to the physical optics calculation in the original design. The advantage of this reverse ray tracing and physical optics procedure is the avoidance of the complexity of the feed geometry and phasing which have only a secondary effect on the results.

Let us consider the hyperbolic reflector to be described by the function

$$f(x,y,z) = (\frac{x}{a} + 1)^2 - \frac{y^2 + z^2}{b^2} - 1 = 0 \tag{3}$$

where y and z are in the domain D of values. If the direction of scan is given by the unit vector $\hat{r}$, then the angle of incidence θ_o with the reflector at the point (x,y,z) on the reflector is obtained from

6

$$\hat{r} \cdot \frac{\nabla f}{|\nabla f|} = \cos \theta_o \tag{4a}$$

and

$$\hat{r} \times \frac{\nabla f}{|\nabla f|} = - \hat{t} \sin \theta_o \tag{4b}$$

where $\hat{t}$ is a unit vector parallel to the surface. For z equal to zero and

$$\hat{r} = \hat{x} \cos\phi + \hat{y} \sin\phi \tag{5}$$

we obtain

$$\frac{\left(\dfrac{x}{a} + 1\right) \dfrac{\cos\phi}{a} - \dfrac{y \sin\phi}{b^2}}{\left[\dfrac{1}{a^2} \left(\dfrac{x}{a} + 1\right)^2 + \dfrac{y^2}{b^4}\right]^{1/2}} = \cos \theta_o \tag{6a}$$

and

$$\frac{\left(\dfrac{x}{a} + 1\right) \dfrac{\sin\phi}{a} + \dfrac{y \cos\phi}{b^2}}{\left[\dfrac{1}{a^2} \left(\dfrac{x}{a} + 1\right)^2 + \dfrac{y^2}{b^4}\right]^{1/2}} = \sin \theta_o \tag{6b}$$

To obtain the effects of the coating, we model the dielectric coated reflector by the locally planar structure shown in Fig. 1. The angle θ_1 is given by Snell's law as

$$\sin \theta_1 = \frac{k_o}{k} \sin \theta_o \tag{7}$$

7
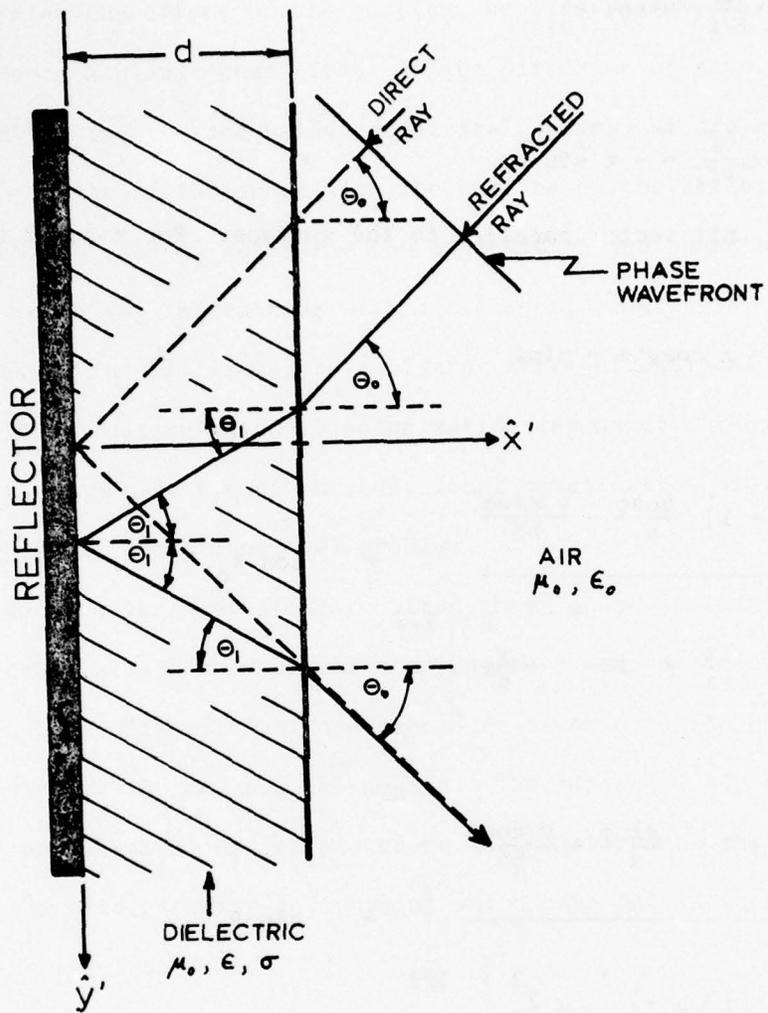
Figure 1. Local Geometry of the Dielectric Coated Reflector

where $k = \epsilon_r(1-j \tan\delta)^{1/2} k_o$, $k_o = 2\pi/\lambda$, ϵ_r is the dielectric constant of the coating, and $\tan\delta$ is the coating loss tangent. This boundary value problem is easily solved by matching the tangential components of the electric and magnetic fields [Jordan and Balmain, 1968]. The resultant change in amplitude and phase of the refracted ray as compared to the direct ray is

$$B_H = \frac{j\frac{\eta}{\cos\theta_1} \tan(kd \cos\theta_1) - \frac{\eta_o}{\cos\theta_o}}{j\frac{\eta}{\cos\theta_1} \tan(kd \cos\theta_1) + \frac{\eta_o}{\cos\theta_o}} e^{j2 k_o d \cos\theta_o} \tag{8}$$

for horizontal polarization ($\overline{E}$ parallel to $\hat{z}$) and

$$B_V = \frac{j\eta\cos\theta_1\tan(kd \cos\theta_1) - \eta_o\cos\theta_o}{j\eta\cos\theta_1\tan(kd \cos\theta_1) + \eta_o\cos\theta_o} e^{j2k_o d \cos\theta_o}$$

for vertical polarization ($\overline{E}$ in the x – y plane) where $\eta = \eta_o/[\epsilon_r(1-j \tan\delta)]^{\frac{1}{2}}$ and $\eta_o = 120\pi$.

To obtain the antenna pattern we compute

$$P = \left| A \int_{y_1}^{y_2} (\hat{r} \times \overline{J}_{s\binom{H}{V}}) B_{\binom{H}{V}} e^{jk\hat{r}\cdot\overline{r}'} \sqrt{1 + \left(\frac{dx'}{dy'}\right)^2}\, dy' \right| \tag{10}$$

A double-primed coordinate system is chosen as shown in Fig. 2, where $\hat{x}''$ equals the scan direction and α is the angle of the elevation pattern with respect to the scan direction. The above integral is approximated by

$$P_{\binom{H}{V}} = C \left| \int_{y_1'}^{y_2'} B_{\binom{H}{V}} e^{jky''\sin\alpha} dy'' \right|. \tag{11}$$
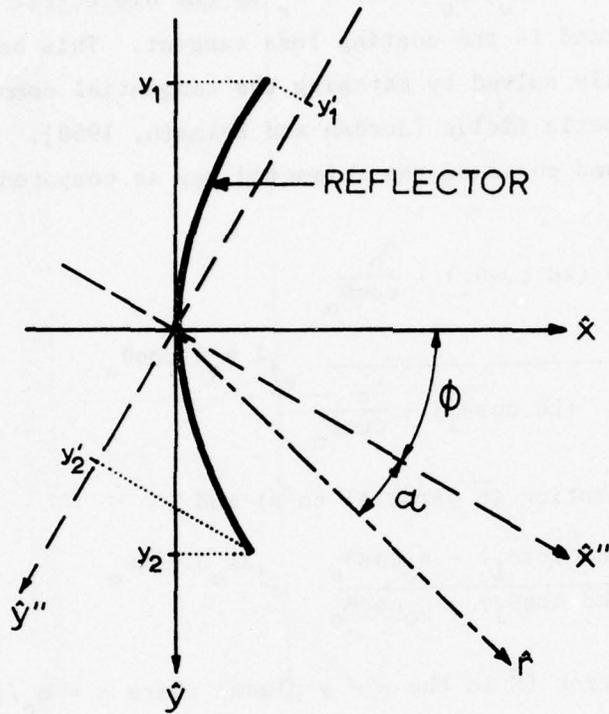
Figure 2. Coordinate Rotation for Pattern Computation

This is just the inverse Fourier transform of B_H or B_V non-zero over the range y_1' to y_2'. The transform variable is $k\sin\alpha$. The validity of the approximation is based upon both ϕ and α being relatively small and the effective aperture from y_1' to y_2' being assumed to be uniformly illuminated.

The simplest method of obtaining this antenna pattern which is a Fourier transform is by the use of the FFT (fast-Fourier-transform) algorithm on the computer. Therefore, 512 uniform samples of y'' are projected onto the reflector by geometrical optics to calculate B_H and B_V for rays intersecting the reflector and setting $B_H = B_V = 0.0$ for rays not intersecting the reflector. A function B_o was also defined as unity for rays intersecting and zero for rays not intersecting the reflector. The resultant patterns, P_H and P_V, are computed by the FFT and plotted. The pattern P_o due to B_o, corresponding to no coating, is also computed and plotted for reference.

The approximation used for the calculation of the patterns is more reasonable when we realize that the true pattern is easily obtained by convolving the inverse Fourier transform of the neglected feed effect with the already computed pattern function in magnitude and phase.

2.3 INTEGRATED CANCELLATION RATIO.

The integrated cancellation ratio (ICR) is a measure of the degree of precipitation - clutter suppression by a circularly - polarized radar system incorporating a suppression technique. For the purposes of this paper, it suffices to consider it as the degree of circular polarization integrated over the antenna pattern. From the form given by Offutt, etal (Jasik, 1961), we have

$$ICR = \frac{\int_s (\text{Pwr received})ds}{\int_s (\text{Pwr returned})ds}$$

for a radar system in the presence of symmetrical objects. If we define an effective length $\overline{h}(0,\phi)$ of the antenna, the power received with suppression is

$$P_{rcv} = C|\overline{h}\cdot\overline{h}|^2$$

11

where C is a constant, and the power returned is

$$P_{ret} = C|\overline{h} \cdot \overline{h}^*|^2$$

The resultant ICR is given by

$$ICR = \frac{\int_s |\overline{h} \cdot \overline{h}|^2 \sin\theta d\theta d\phi}{\int_s |\overline{h} \cdot \overline{h}^*|^2 \sin\theta d\theta d\theta}$$

In measurements it is more common to describe ICR in terms of the maximum and minimum one-way received power from a linearly polarized antenna versus polarization. The resultant form is

$$ICR = \frac{\int_s (P_{max} - P_{min})^2 \sin\theta d\theta d\phi}{\int_s (P_{max} + P_{min})^2 \sin\theta d\theta d\phi} .$$

This last form is the one which has been modified to determine the ICR in our problem.

We recognize two simplifications. First, the problem is two-dimensional and thus the θ integration way be eliminated. The second simplification is to assume that the field is negligible far from the main beam and thus it is sufficient to integrate in a small domain enclosing the main beam (domain width used was about 0.8 radians). Thus the ICR becomes

$$ICR = \frac{\sum\limits_{Sector} (P_{max} - P_{min})^2}{\sum\limits_{Sector} (P_{max} + P_{min})^2}$$

and is the form used for the computation in Chapter 3.

12

2.4 DIELECTRIC CHARACTERISTICS.

To complete the analysis, we must have a model of the dielectric coating of interest. Although typical properties of ice are readily available in several references, it was desired to obtain more detailed information. A paper by S. Evans [1965] provides just the type of material required. This paper reviews the measurements made of ice and snow properties in audio through radio frequencies.

The data presented by Evans agrees with a relative permittivity (dielectric constant) of ice found in engineering handbooks of 3.2 while the loss tangent is small at about 3×10^{-4}. Both the dielectric constant and loss tangent are found to have only minor variations with temperatures below freezing. Above freezing, however, the effect of loss in the surface water due to melting increases the loss tangent substantially. It is also assumed that ice and snow have negligible magnetic properties and thus a unity relative permability ($\mu = \mu_o$).

Unlike ice, which has a rather fixed density and minimal water content, snow has both varying degrees of density and wetness. The loss tangent varies from that of an ice/air mixture to that of water which may approach 2 at X - band. The range of interest was chosen to be 0.002 to 0.5. The dielectric constant is almost proportional to the density, varying from 0.0 to 3.2. It should be noted that the crystalline structure of the snow has very little effect on the dielectric constant.

To model the geometry of the dielectric layer, it was assumed that the ice/snow collects only on the lower portion of the reflector (y > 0). On this lower portion, the thickness in the y direction was assumed to be constant. This vertical depth is used to specify the dielectric geometry depth in the next chapter as shown in Fig. 3.

The effects of a rough dielectric surface was not considered since typical roughness is much less than a wavelength, averaging to zero, and the effects of a smooth dielectric where sufficiently severe as to negate the problems of the rough surface. However the effects of roughness would cause dispersion which has a similar effect on the main beam as would loss.

13
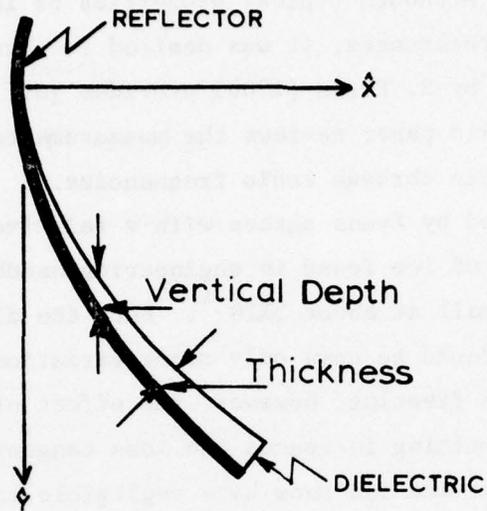
Figure 3. Geometry of the local dielectric thickness and the vertical depth.

3.0 DEGRADATION OF GPN-XX AND TPN-19 ANTENNA PATTERNS

The specific purpose of this report is to obtain estimates of the pattern degradation of both the GPN-XX and the TPN-19 PAR antenna systems. In this chapter we apply the analysis procedure of the previous chapter to both antenna systems with various thicknesses and characteristics of ice and snow coatings.

3.1 GPN-XX ANALYSIS

The GPN-XX is a high power, fixed, airport radar system. The vertical geometry of the PAR reflector is shown in Fig 4. The quantities defining the reflector surface are given in inches for Eq. 3 as a = 162.10" and b = 216.82" (or b^2 = 47,010). The equation of the surface is thus

$$\left(\frac{x}{162.10} + 1\right)^2 - \frac{y^2+z^2}{47,010} - 1 = 0. \tag{12}$$

This reflector is used for elevation scan angles between -1° and 7° with a precision sector of 0° to 4°. In accordance with the geometry of Fig. 4, ϕ would vary from 16.5^o to 8.5^o for these scan angles ($\phi = 15.5^o$ = horizontal scan angle).

Worst case examples were used in the computer program. This included the extreme scan angles, the extremes of loss tangents, and two depths of ice or snow. Hence, for wavelength of 1.297 inches (9.1 GHz), the angle ϕ was 8.5 or 16.5 degrees, the loss tangent was 0.002, 0.05, or 0.5, and the vertical depth shown in Fig. 3 was 1.0 or 4.0 inches. A parameter study was also made of the beamshift and integrated cancellation ratio (ICR) versus dielectric depth. For all of these cases, the dielectric constant was set to the value of 3.2.

The results were found to be relatively independent of the scan angle, though inclusion of the actual feed would show an effect due to the partial illumination of the reflector. The effect of the loss tangent was to lower the beam amplitude while having a negligible effect on the shift in beam position as shown in Figs. 5 and 6 for a 4 inch vertical dielectric depth. The dielectric thickness at the reflector varied almost linearly from 0.0 inches at the center to 1.53 inches at

15
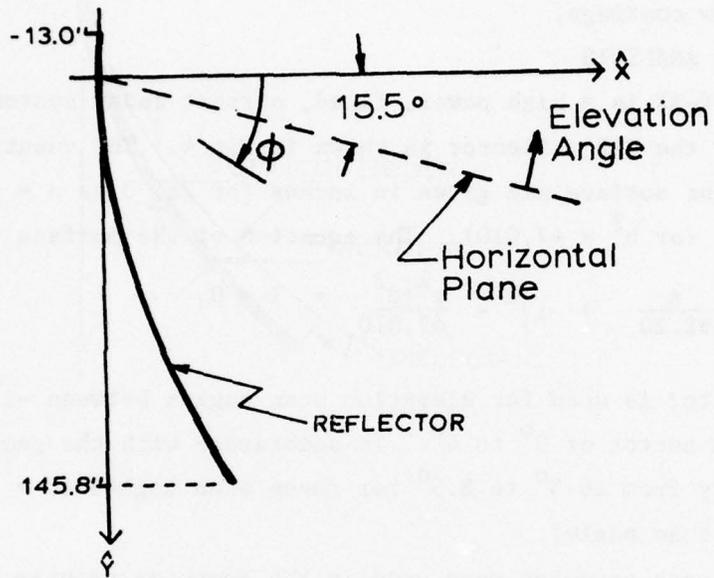
Figure 4. Sideview of GPN-XX PAR Antenna Reflector Geometry
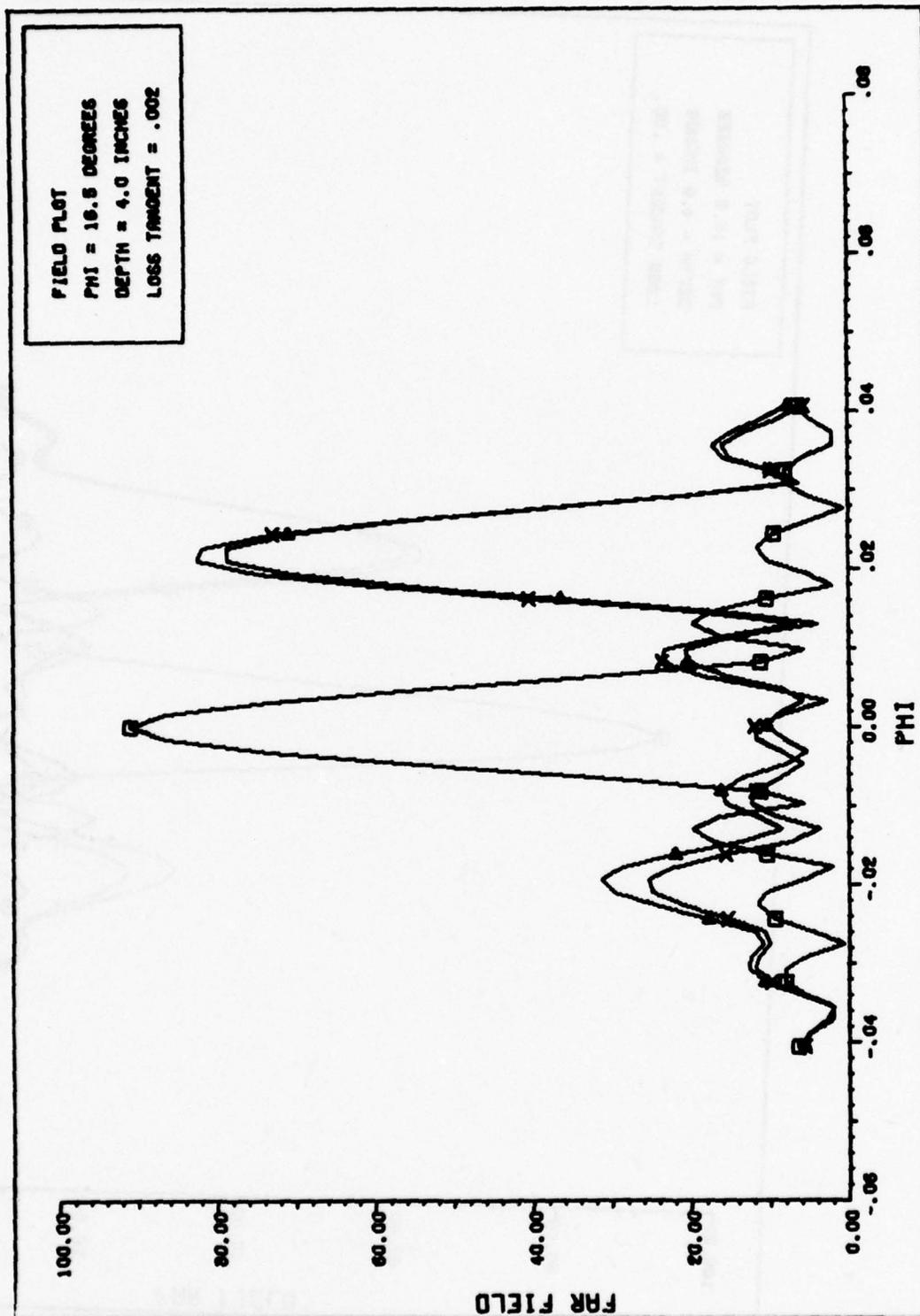
Figure 5. The GPN-XX pattern with no coating (□) and with a four inch depth dielectric having a dielectric constant of 3.2 and a loss tangent of 0.002 at a wavelength of 1.297 inches. (Vertical = x, horizontal = Δ)

17
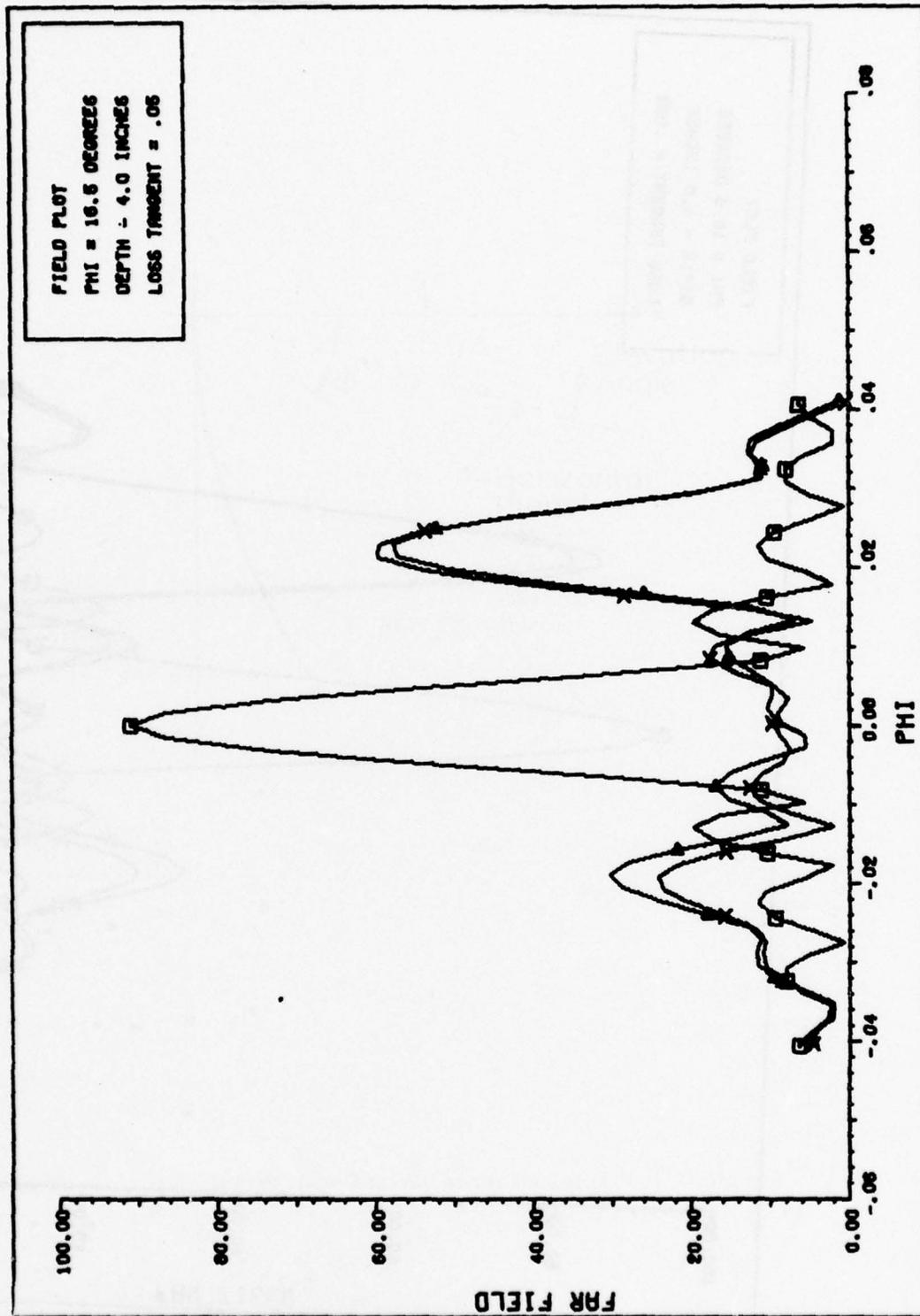
Figure 6. The GPN-XX pattern with no coating (□) and with a four inch depth dielectric having a dielectric constant of 3.2 and a loss tangent of 0.05 at a wavelength of 1.297 inches. (Vertical = x, horizontal = Δ)

the bottom as shown in Fig. 7.

If the loss tangent is 0.5, the pattern is nullified in Fig. 8. Measurements by Cumming [Evans, 1965] show loss tangents less than .05 for snow with free water content less than 1.6 percent in two snow samples. This should generally be adequate water content to lower the sliding friction at the reflector sufficiently to clear the reflector of snow and thus the associated high loss problem. As a result, the effects of loss may be neglected and consideration only be given to the beamshift.

Parametric studies of the beamshift and integrated cancellation ratio are presented respectively in Figs. 9 and 10 versus the vertical dielectric depth.

3.2 TPN-19 ANALYSIS

The TPN-19 is a portable version of the GPN-XX (TPN-19 actually designed first). The primary differences in the antenna system are the directly illuminated transmission elements in the feed rather than a reflection illuminated system in addition to a rotation of the antenna system by 90°. The resultant side feed reflector is the reason for the difficulty in analysis. These difficulties were ignored and conservative estimates obtained using the same theory as for the GPN-XX with the assumption that z is zero in the reflector equation. The geometry of a vertical cross-section is given in Fig. 11. The corresponding equation is

$$\left(\frac{x}{200} + 1\right)^2 - \frac{y^2+z^2}{36,000} - 1 = 0. \tag{13}$$

This antenna system is designed for a vertical scan of -1.0° to 14.0° with respect to the horizontal. The corresponding range for ϕ is from 6.0° to -9.0°.

The same cases have been evaluated as for the GPN-XX. A plot of the dielectric thickness for a four inch vertical depth is shown in Fig. 12. The results however show a substantially different effect. In Fig. 13, the low loss, four inch depth for $\phi = 6.0^{\circ}$ shows a dual beam effect with beams located at approximately 0.0 and 30.0 milliradians. The rather broad beams result from the upper half and the lower coated half of the reflector respectively. This is even more evident as we look at the
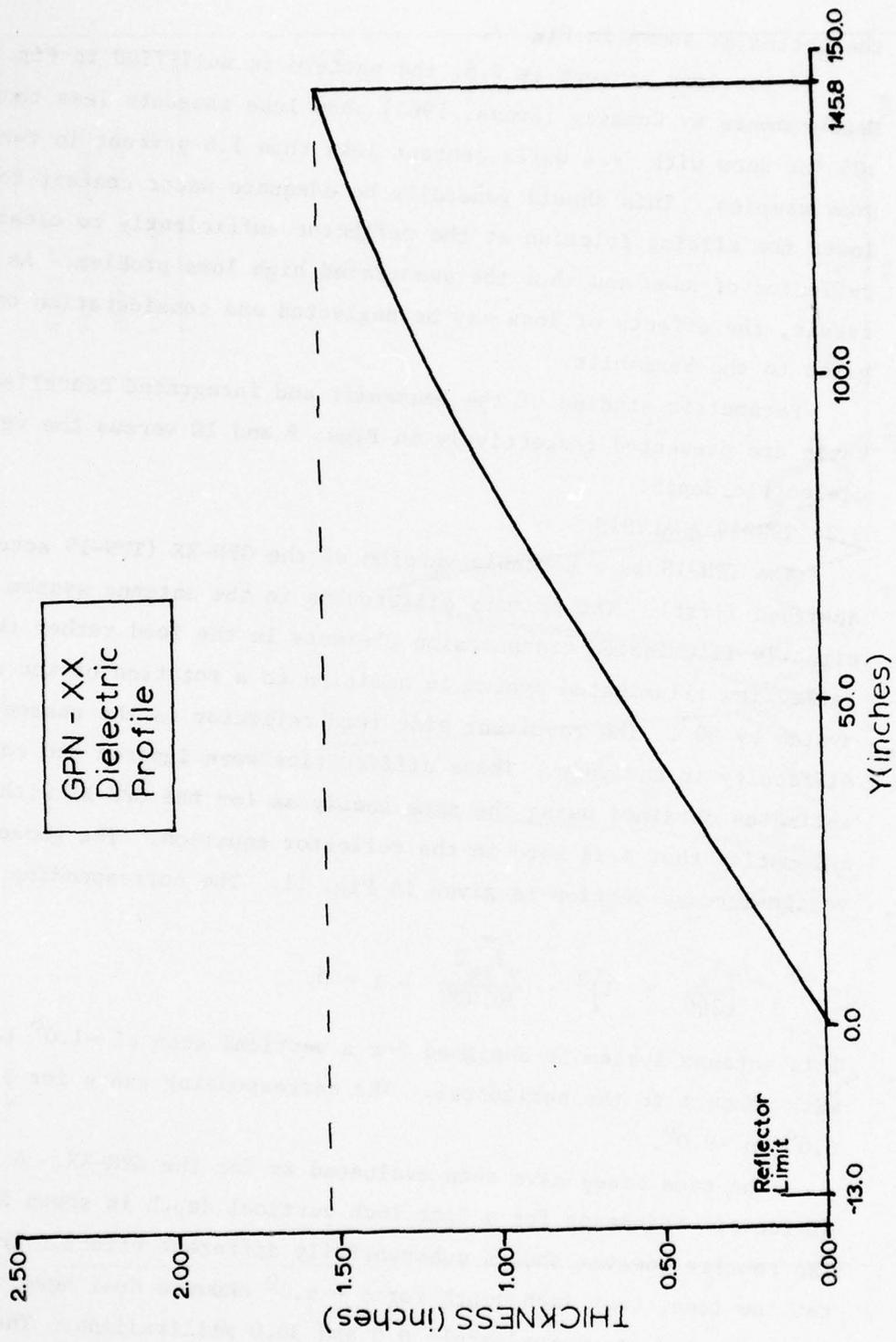
Figure 7. Thickness profile of the dielectric coating on the GPN-XX for a four inch vertical depth.
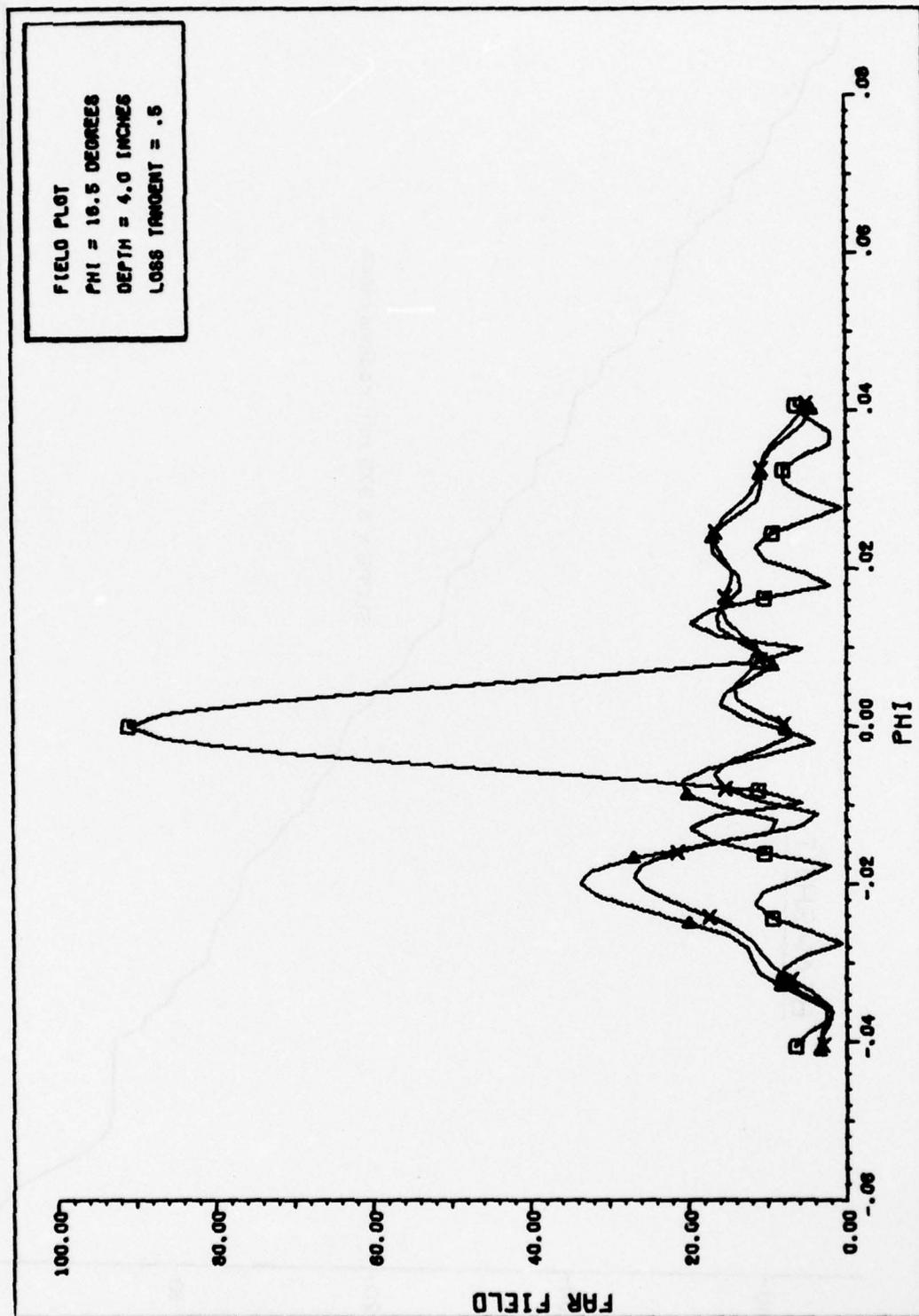
Figure 8. The GPN-XX pattern with no coating (□) and with a four inch depth dielectric having a dielectric constant of 3.2 and a loss tangent of 0.5 at a wavelength of 1.297 inches. (Vertical = x, horizontal = Δ)

21
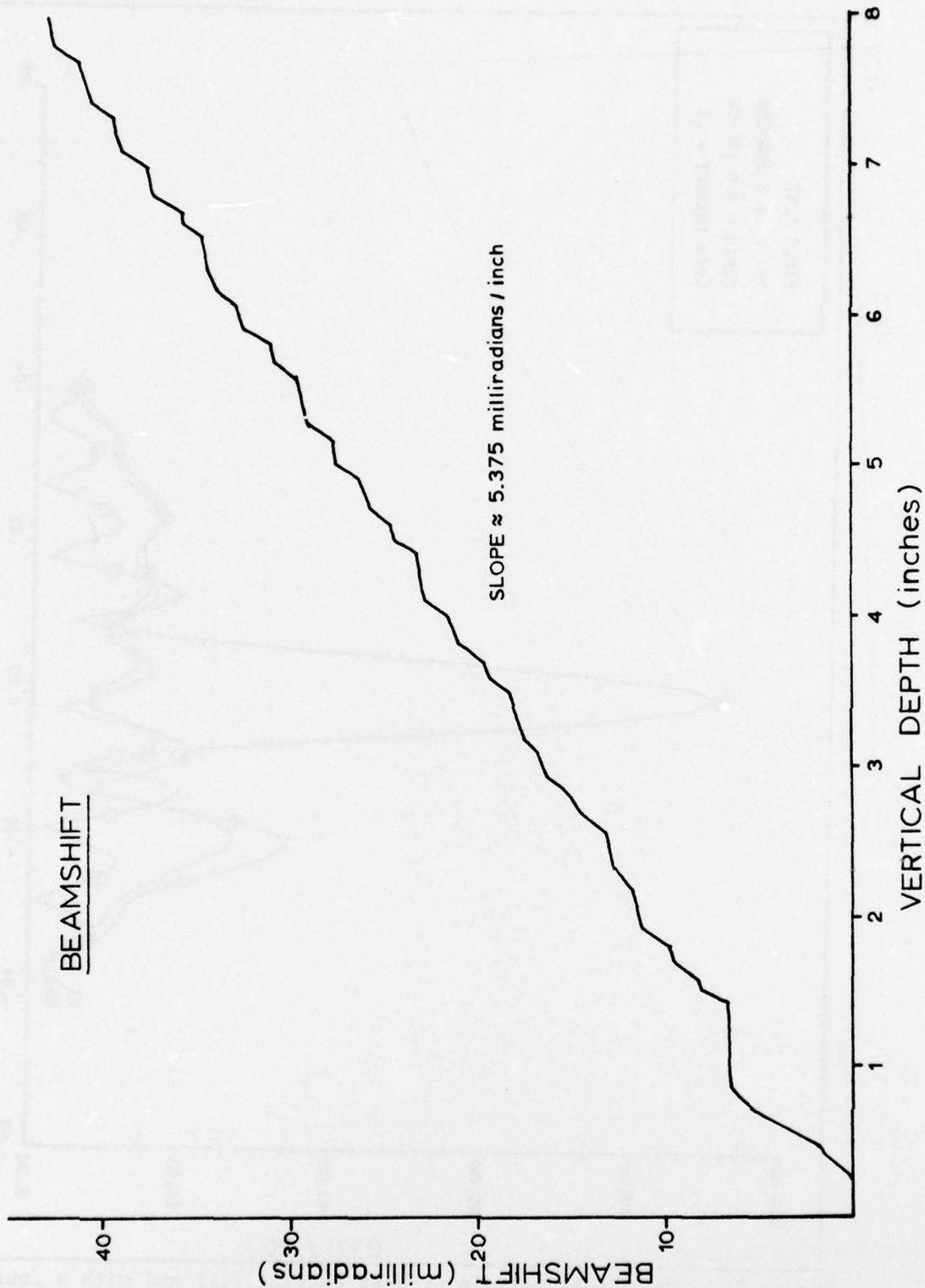
Figure 9. Beamshift of the GPN-XX main beam versus vertical depth of a lossless dielectric with a dielectric constant of 3.2 (ice) at a wavelength of 1.297 inches (9.1 GHz). Elevation angle = $15.5^o - \phi$.

22
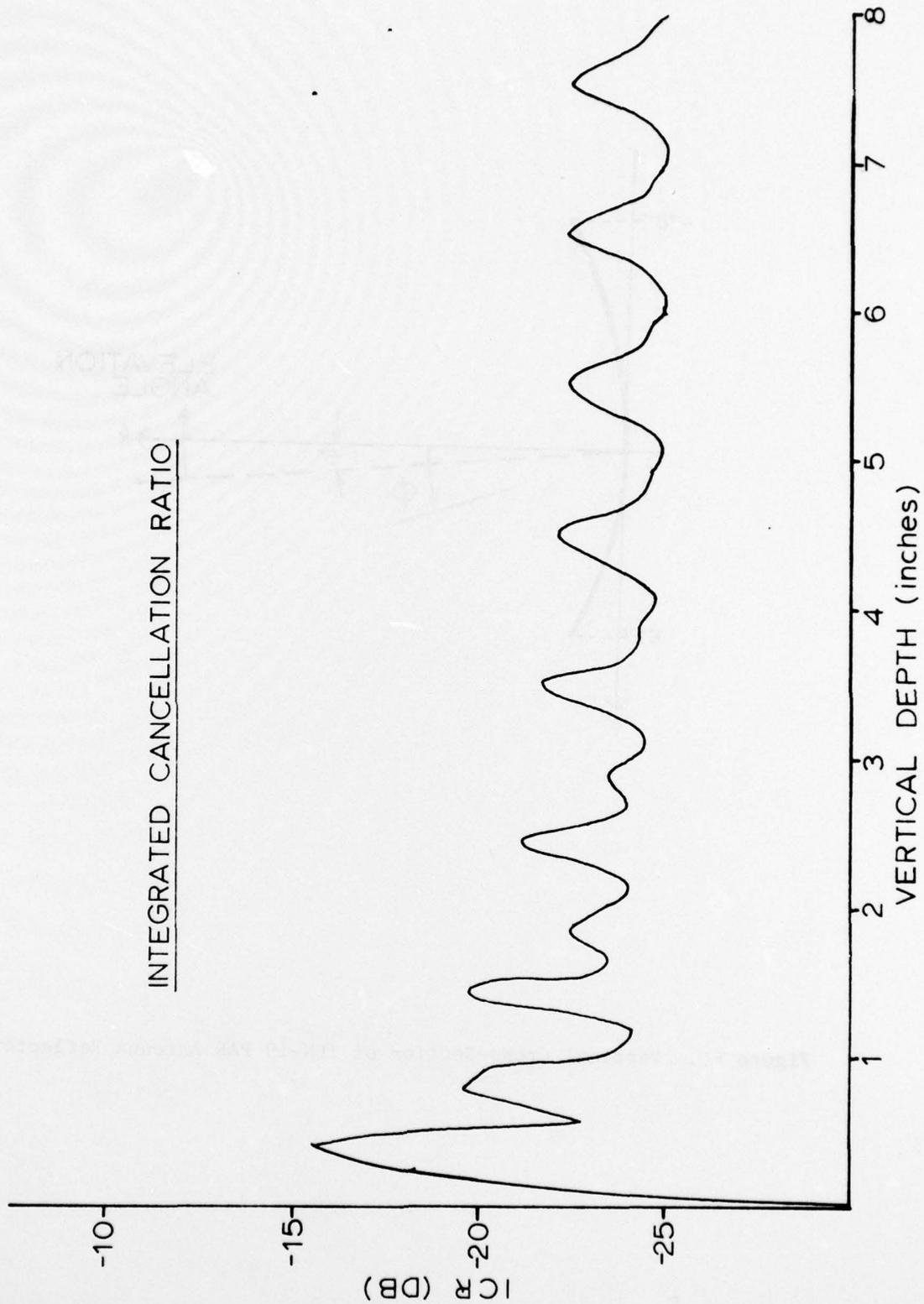
Figure 10. Integrated cancellation ratio due only to a dielectric coating on the GPN-XX reflector versus vertical depth of a lossless dielectric with a dielectric constant of 3.2 (ice) at a wavelength of 1.297 inches (9.1 GHz). Elevation angle = 15.5° - φ.
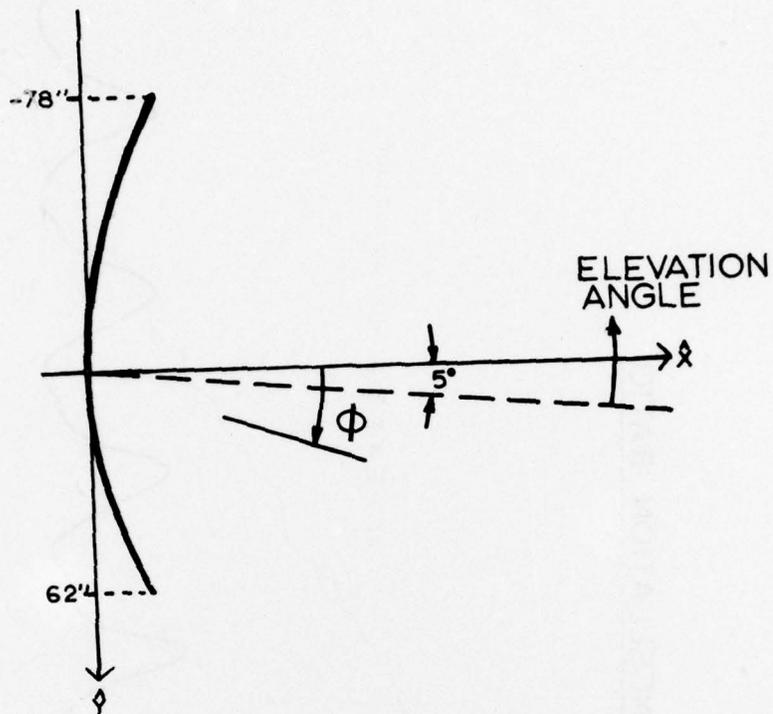
Figure 11. Vertical Cross-Section of TPN-19 PAR Antenna Reflector
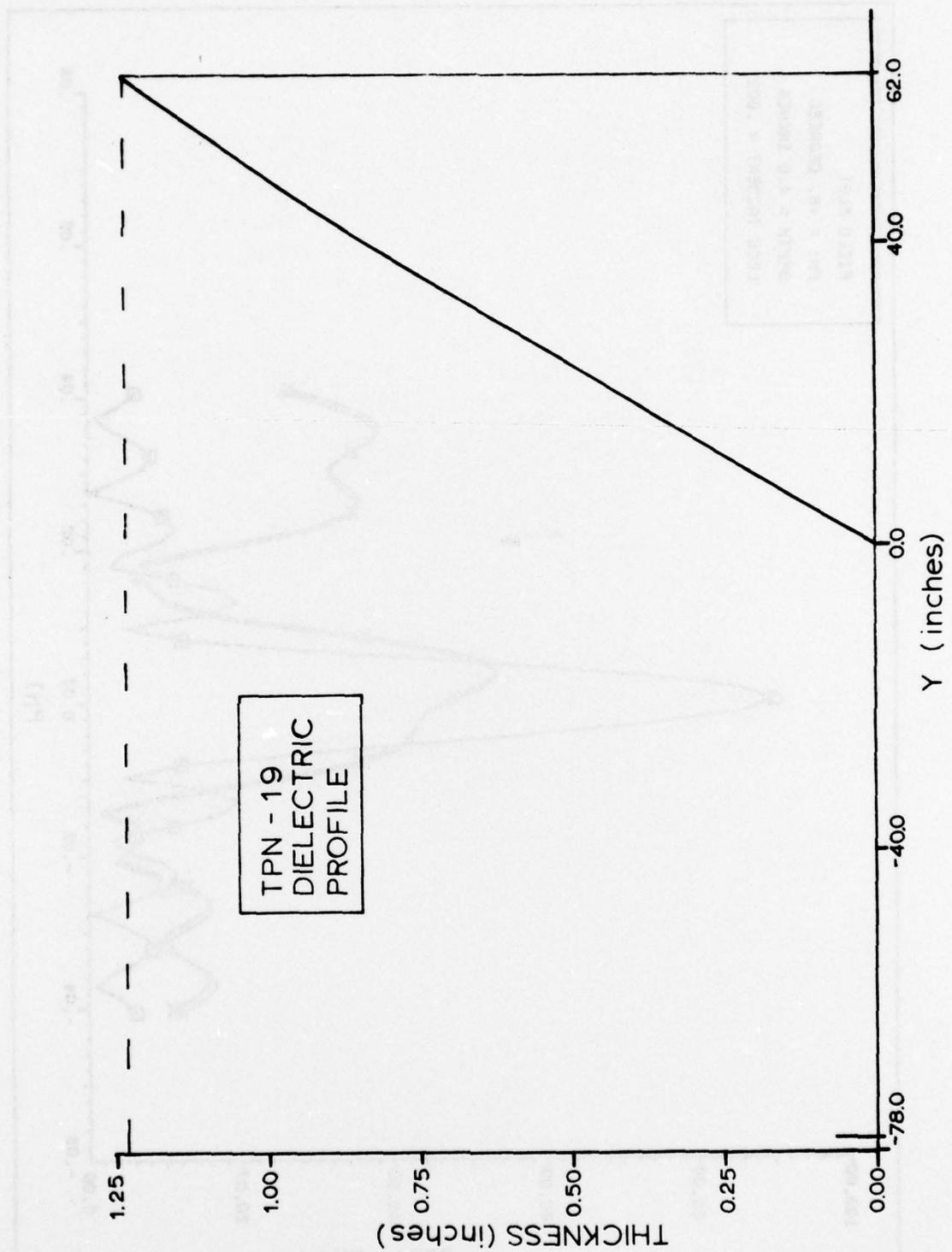
Figure 12. Thickness profile of the dielectric coating on the TPN-19 for
a four inch vertical depth.

25
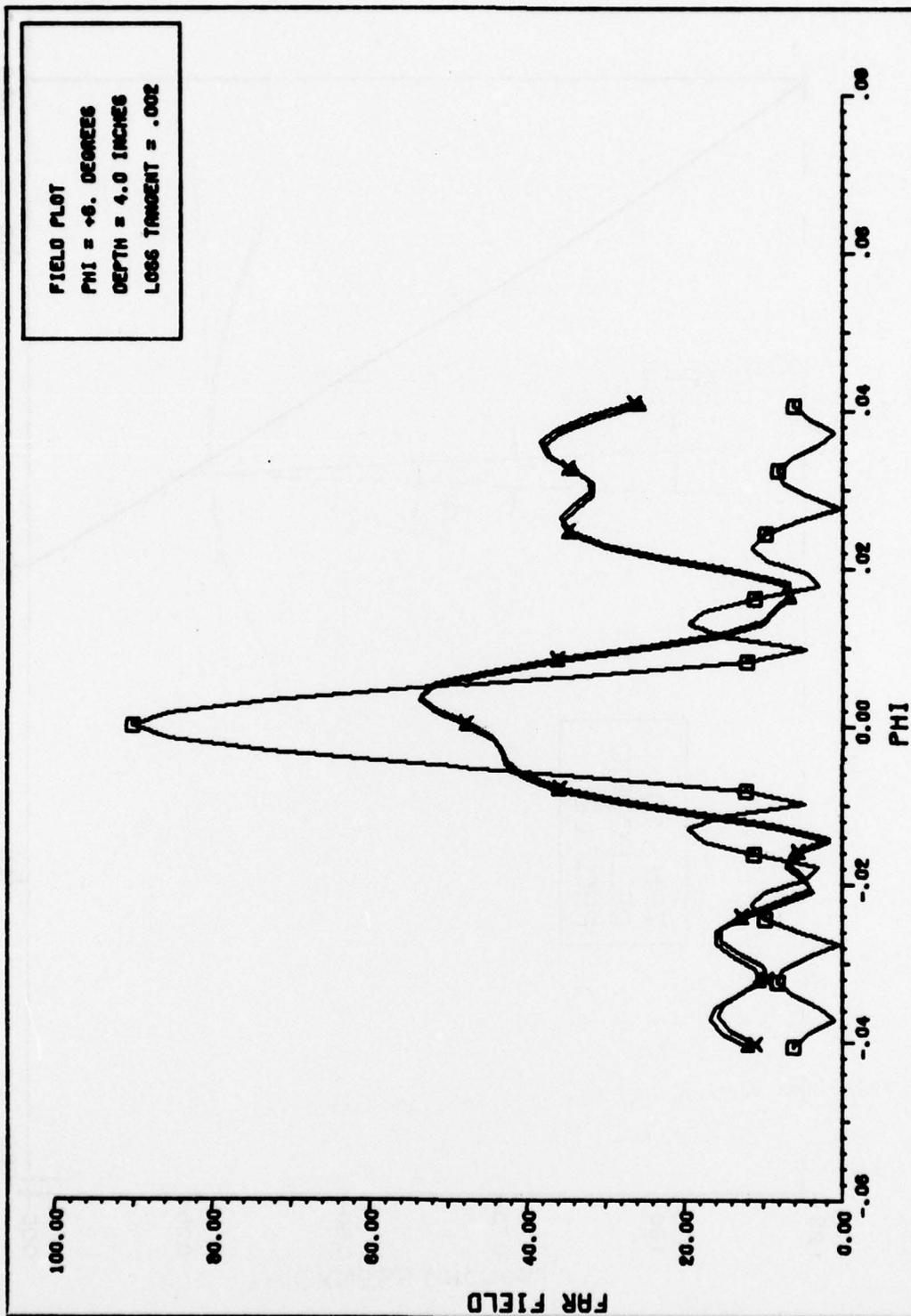
Figure 13. The TPN-19 pattern with no coating (□) and with a four inch depth dielectric having a dielectric constant of 3.2 and a loss tangent of 0.002 at a wavelength of 1.297 inches. (Vertical = x, horizontal = Δ.

higher loss cases of Figs. 14 and 15 to see the beam at 30.0 milliradians nullified by the loss while the beam at 0.0 milliradians remains with roughly twice the beamwidth of the original. As with the GPN-XX, one should not expect the loss tangent to rise above 0.05 and it is sufficient to consider the beam shift due to the dielectric constant only.

The results of parametric studies versus depth of dielectric are shown in Figs. 16 and 17 for the beamshifts and integrated cancellation ratio respectively. It is noted that the dual beam effect appears with between a one and two inch depth (order of one wavelength) of ice. The ICR is within the 20DB specification by 15 to 20 DB. This should cause only minor changes to the overall ICR of the system.
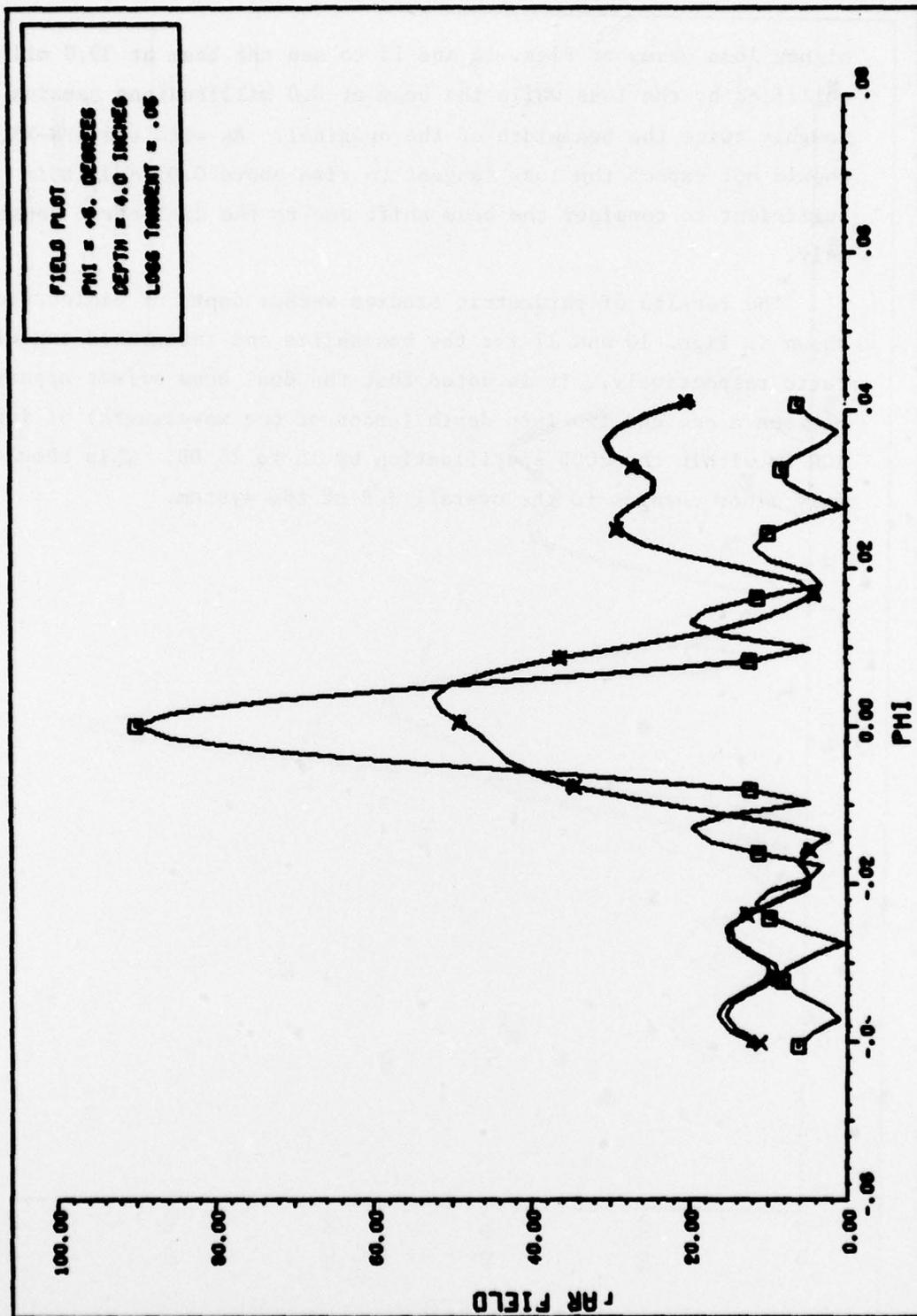
Figure 14.   The TPN-19 pattern with no coating (□) and with a four inch
            depth dielectric having a dielectric constant of 3.2 and a
            loss tangent of 0.05 at a wavelength of 1.297 inches.
            (Vertical = x, horizontal = Δ)
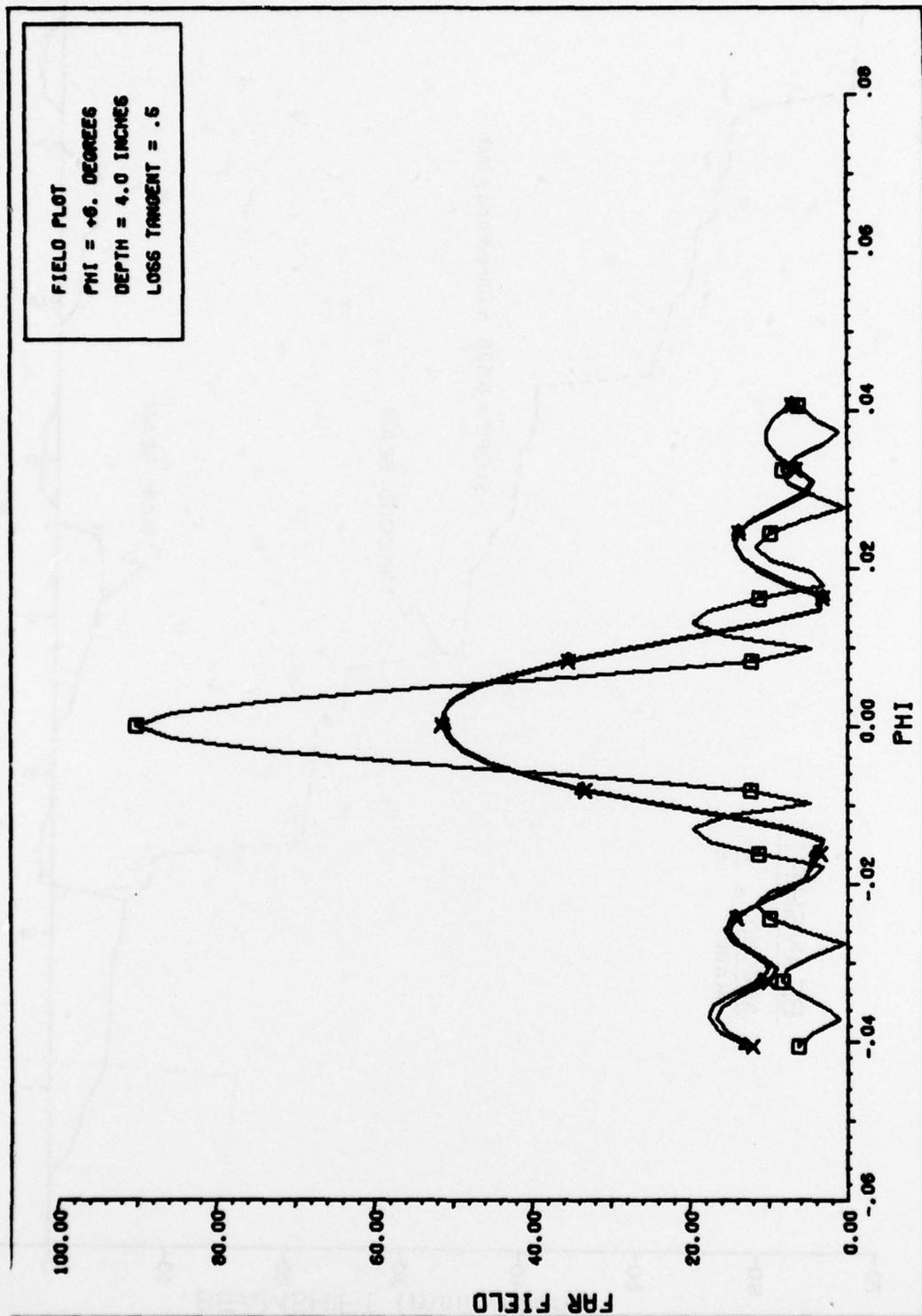
Figure 15. The TPN-19 pattern with no coating (□) and with a four inch depth dielectric having a dielectric constant of 3.2 and a loss tangent of 0.5 at a wavelength of 1.297 inches. (Vertical = x, horizontal = △.
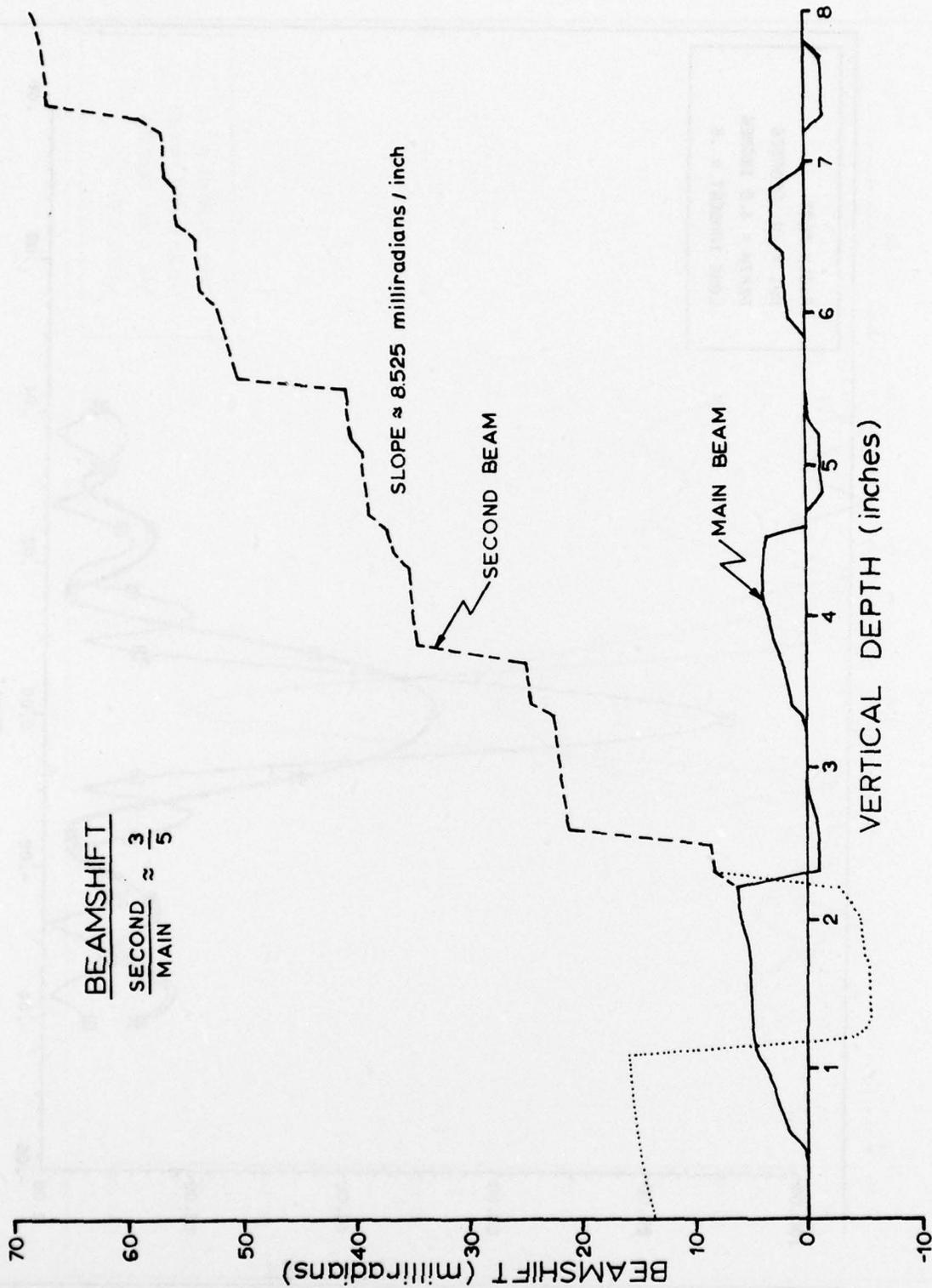
Figure 16. Beamshift of the TPN-19 main beam versus vertical depth of a lossless dielectric with a dielectric constant of 3.2 (ice) at a wavelength of 1.297 inches (9.1 GHz). Elevation angle = $5.0^\circ - \phi$.

30
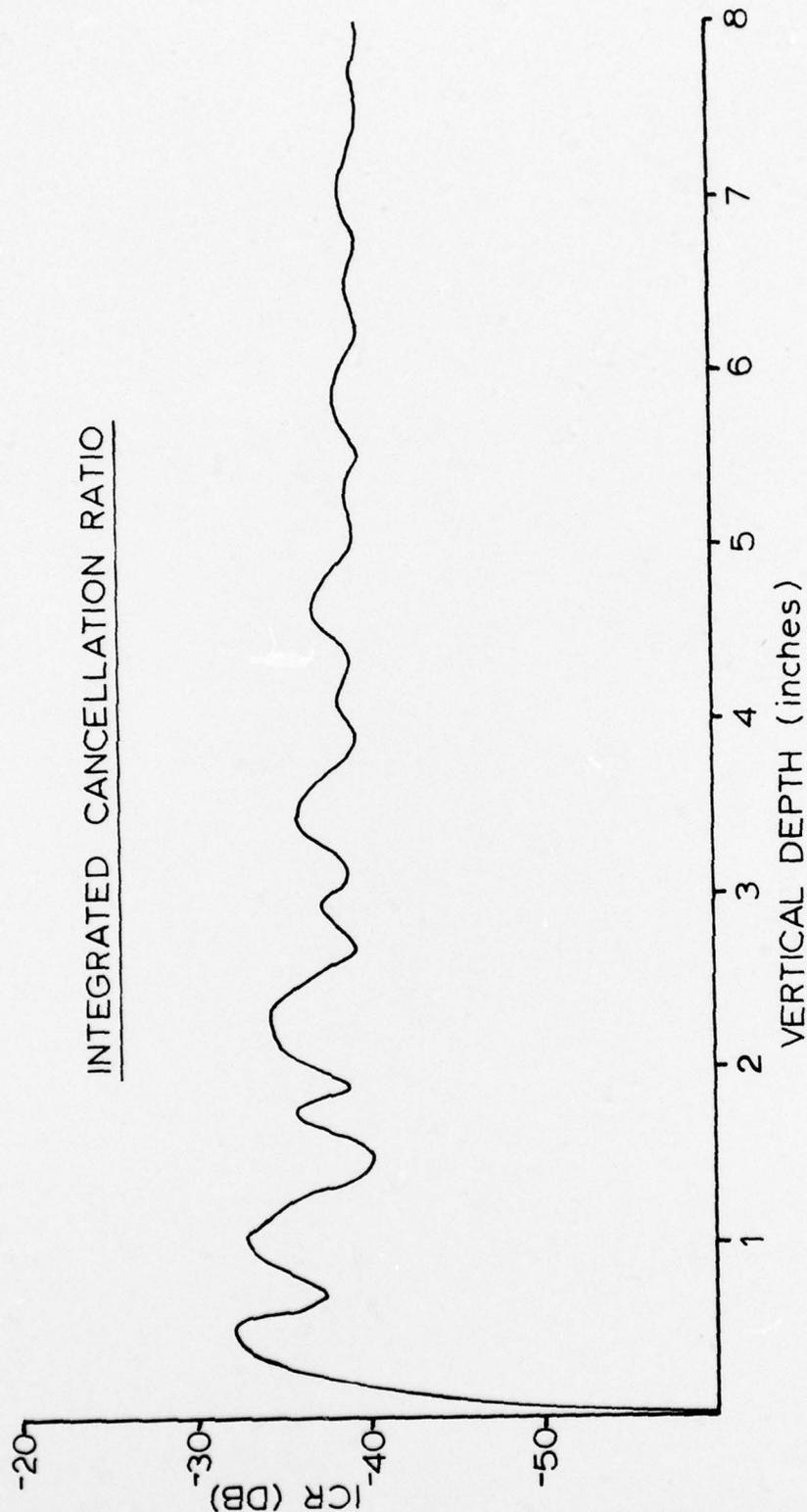
Figure 17. Integrated cancellation ratio due only to a dielectric coating on the GPN-XX reflector versus vertical depth of a lossless dielectric with a dielectric constant of 3.2 (ice) at a wavelength of 1.297 inches (9.1 GHz). Elevation angle = $5.0^{\circ} - \phi$.

31

4.0 CONCLUSIONS

This study has used the theories of geometrical optics and physical optics to develop a two-dimensional analysis of reflector antennas for the evaluation of vertical beamshifts due to ice or snow buildup on the reflector surface. The analysis is based on the design of the GPN-XX and TPN-19 PAR antenna systems by Raytheon.

The beamshifts were found to be downward in elevation as also had been concluded by previous investigators. The effect of extreme loss is to decrease the useable reflector area. For the GPN-XX, the total reflector is lost, whereas only the lower half of the TPN-19 losses effectiveness. However, the slope of the reflectors is sufficient to generally clear the reflectors of the slush characteristic of high loss ice and snow by lowering the coefficient of friction at the surface. As a result, the effects of loss are negligible. The estimates of beamshifts indicate that as little as one quarter wavelength average thickness of ice with an approximate linear slope on the reflector will cause downward beamshifts of about ten (10) milliradians with a dual beam on the TPN-19 due to its half ice coating.

REFERENCES

Evans, S. (1965), "Dielectric Properties of Ice and Snow - a Review," memo to ESD/OCNG.

Jasik, H., ed. (1961), Antenna Engineering Handbook, pp 17:22-24, McGraw-Hill, N. Y.

Jordan, E. C. and K. G. Balmain (1968), Electromagnetic Waves and Radiating Systems, 2 ed, Prentice-Hall, Englewood Cliffs, N. J.

Kouyoumjian, R. G. (1965), "Asymptotic High-Frequency Methods," Proceedings of the IEEE, pp 865-876, N. Y.

Mailloux, R. J. (1976), "Monopulse Pattern Degradation due to Monuniform Ice on a Reflector," memo to ESD/OCNG.

Melancon, L. (197X), "A Limited Scan Antenna," Raytheon Company.

Raytheon Company (1975), "Minutes of Critical Design Review for Antenna Group," Raytheon Company.

Tipple, E. (1976), "Effects of Ice on AN/GPN-XX System," memo to ESD/OCNG.

REPORT DOCUMENTATION PAGE	READ INSTRUCTIONS BEFORE COMPLETING FORM

1. REPORT NUMBER AFIT-TR-77-8	2. GOVT ACCESSION NO.	3. RECIPIENT'S CATALOG NUMBER

4. TITLE (and Subtitle) Electrical Effects of Snow and Ice Coatings on Reflector Antennas	5. TYPE OF REPORT & PERIOD COVERED Final Report.
	6. PERFORMING ORG. REPORT NUMBER AFIT TR 77-8

7. AUTHOR(s) William A. Davis	8. CONTRACT OR GRANT NUMBER(s)

9. PERFORMING ORGANIZATION NAME AND ADDRESS Air Force Institute of Technology (AFIT/ENG) Wright-Patterson Air Force Base, OH 45433	10. PROGRAM ELEMENT, PROJECT, TASK AREA & WORK UNIT NUMBERS

11. CONTROLLING OFFICE NAME AND ADDRESS	12. REPORT DATE December 1977
	13. NUMBER OF PAGES 32

14. MONITORING AGENCY NAME & ADDRESS(if different from Controlling Office) Air Force Communications Service (AFSC/XPQ) Scott AFB, Ill.	15. SECURITY CLASS. (of this report) Unclassified
	15a. DECLASSIFICATION DOWNGRADING SCHEDULE

16. DISTRIBUTION STATEMENT (of this Report)

Approved for public release; distribution unlimited

17. DISTRIBUTION STATEMENT (of the abstract entered in Block 20, if different from Report)

18. SUPPLEMENTARY NOTES

Approved for public release; in accordance with AFR 190-17
Jerral F. Guess, Captain, USAF
Director of Information

19. KEY WORDS (Continue on reverse side if necessary and identify by block number)
Reflector Antennas
Icing
Beam Shift
Geometrical Optics

20. ABSTRACT (Continue on reverse side if necessary and identify by block number)

In recent years, the effects of icing on reflector antenna systems used in precision approach radars has become an ever increasing problem of interest. This paper presents a simple technique that may be used for the analysis of the icing on such reflector systems. For simplicity, the ice is assumed to have a uniform vertical thickness over the upper side of exposed surfaces.

DD FORM 1473 EDITION OF 1 NOV 65 IS OBSOLETE
1 JAN 73

012200 B

20. Continued

Beginning with a uniform phase front in the beam direction for the uniced reflector, one can trace rays back to the reflector using geometrical optics to determine the angle of incidence at each point on the reflector. The phase and amplitude of the rays for the iced reflector are computed by local plane wave analysis and used to calculate the far field in the manner of physical optics. This technique gives downward beam shifts of up to 30 milliradians for some typical reflectors.

This technique modifies the array aperture function. The full pattern can obtained from the convolution of the computed pattern with the pattern of the original system.